

TRIGGERED STAR FORMATION IN THE ORION BRIGHT-RIMMED CLOUDS

Hsu-Tai Lee¹

eridan@astro.ncu.edu.tw

W. P. Chen^{1,2}

wchen@astro.ncu.edu.tw

Zhi-Wei Zhang¹

and

Jing-Yao Hu³

ABSTRACT

We have developed an empirical and effective set of criteria, based on the 2MASS colors, to select candidate classical T Tauri stars (CTTS). This provides a useful tool to study the young stellar population in star-forming regions. Here we present our analysis of the bright-rimmed clouds (BRCs) B 35, B 30, IC 2118, LDN 1616, LDN 1634, and Orion East to show how massive stars interact with molecular clouds to trigger star formation. Our results support the radiation-driven implosion model in which the ionization fronts from OB stars compress a nearby cloud until the local density exceeds the critical value, thereby inducing the cloud to collapse to form stars. We find that only BRCs associated with strong IRAS 100 μ m emission (tracer of high density) and H α emission (tracer of ionization fronts) show signs of ongoing star formation. Relevant timescales, including the ages of O stars, expanding HII regions, and the ages of CTTS, are consistent with sequential star formation. We also find that CTTS are only seen between the OB stars and the BRCs, with those closer to the BRCs being progressively younger. There are no CTTS leading the ionization fronts, i.e.,

¹Institute of Astronomy, National Central University, Taiwan 320, R.O.C.

²Department of Physics, National Central University, Taiwan, 320, R.O.C.

³National Astronomical Observatories, Chinese Academy of Sciences, Beijing 100012, People's Republic of China.

within the molecular clouds. All these provide strong evidence of triggered star formation and show the major roles massive stars play in sustaining the star-forming activities in the region.

Subject headings: stars: formation — stars: pre-main sequence — ISM: clouds
— ISM: molecules

1. INTRODUCTION

Young stars tend to form in clusters or groups. A giant molecular cloud may collapse and fragment to form stars of different masses. The formation of massive stars has an immense impact on the environments. On one hand stellar winds and shock waves from a supernova explosion may squeeze molecular clouds and induce subsequent birth of stars which otherwise may not have occurred. On the other hand the agitation may be so violent as to disperse the material, hindering further star-forming activity. Triggered star formation (see Elmegreen 1998, for a comprehensive review) — as opposed to spontaneous cloud collapse — would have profound consequences in stellar population, chemical homogeneity, star formation efficiency, and cloud energetics.

While the OB and young low-mass member stars are often distributed cospatially, in some cases low-mass pre-main-sequence (PMS) stars are seen to be located between the molecular cloud and the cluster. Such a configuration can result from either triggered or spontaneous star formation. In the former case, high-mass stars form in dense molecular cores, and then their UV photons create an expanding Strömgren sphere. The expanding ionization fronts (I-fronts) then compress nearby molecular clouds and trigger the formation of next-generation PMS stars at the edge of clouds. Alternatively, star formation may proceed in a spontaneous way; that is, all stars form coevally but high-mass stars photoionize the surrounding clouds to expose the low-mass stars.

The Orion complex is an active star-forming region with a wealth of star-forming signatures, such as high-mass star clusters, OB associations, low-mass young stars, giant molecular clouds, reflection nebulae and H II regions. Because of its proximity, at ~ 450 pc, it is a suitable laboratory for the study of star formation, especially for the interplay among high-mass stars, low-mass stars, and interstellar medium.

Bright-rimmed clouds (BRCs) are usually found at the boundary of H II regions and the edge of molecular clouds. The morphology of a BRC, e.g., tightly curved or cometary rims with tails, is governed by the I-fronts from nearby OB stars, which compress the head of the BRC, hence making the density of the apex higher than the other parts of the cloud.

The imprints of such causality offer the possibility to delineate the intricate processes of sequential star formation. Sugitani et al. (1991, 1994) catalogue 89 BRCs associated with IRAS point sources in both northern and southern hemispheres, some of which are also associated with Herbig-Haro objects and molecular outflows. These BRCs are potential sites where triggered star formation might have taken place. Karr & Martin (2003) present a multiwavelength study of triggered star formation in the W5 HII region. They find some young stellar objects around W5 and suggest that the expanding HII region has induced star formation in the surrounding molecular clouds.

This paper provides observational diagnosis to identify PMS stars from their characteristic near-infrared colors. In particular, PMS stars associated with BRCs in the Orion star-forming region are used as a tool to chronologize the star formation history to show how massive stars trigger the star formation processes in the region.

We describe in §2 our methodology in selection of the PMS sample in parts of the Orion and Monoceros star-forming regions. In §3 we discuss how our data lend supportive evidence of triggered star formation in the Orion BRCs. The conclusions are summarized in §4.

2. SELECTION OF YOUNG STELLAR SAMPLE

Weak-line T Tauri stars (WTTS) are known to emit copious x-ray emission, and a majority of them have been identified by optical spectroscopic observations of strong x-ray sources (see Feigelson & Montmerle 1999, for a review). In comparison, classical T Tauri stars (CTTS) are at earlier evolutionary stages, before much of the circumstellar material has been dispersed. CTTS show characteristic strong IR excess emission, particularly at mid-infrared wavelengths, and H α emission (equivalent width $> 5 \text{ \AA}$). The IR excess is believed to originate from heated circumstellar dust, whereas the H α emission come from an active chromosphere and the boundary layer between the young star and the fast rotating circumstellar disk. As young stars evolve and gradually clear away the surrounding material, they show different amounts of IR excesses, hence their near-infrared colors (Lada & Adams 1992). Our PMS candidates have been selected on the basis of their near-infrared colors.

2.1. 2MASS AND OTHER DATA

This project started in early 2003, when we used the Two-Micron All-Sky Survey (2MASS) Second Incremental Data Release to identify CTTS candidates in the Orion and Monoceros regions. Since the 2MASS released their All-Sky Data in March 2003, we have

updated the photometry of our sample accordingly. The 2MASS database provides unbiased photometry in the near-infrared J ($1.25 \mu\text{m}$), H ($1.65 \mu\text{m}$), and K_S ($2.17 \mu\text{m}$) bands to a limiting 15.8, 15.1, and 14.3 mag, respectively, with a signal-to-noise ratio (SNR) greater than 10. The comprehensive database offers a good opportunity to identify in a systematic way young star candidates associated with molecular clouds. We use known WTTS (Wichmann et al. 1996), CTTS (Herbig & Bell 1988) and Herbig Ae/Be stars (Thé et al. 1994) as our template to select PMS candidates. These lists of WTTS, CTTS and Herbig Ae/Be stars, taken from the literature and not confined to any special region in the sky, serve to the compilation of their descriptive 2MASS colors. Figure 1 plots the $(J - H)$ versus $(H - K_S)$ color-color diagram, extracted from the 2MASS catalog for these PMS stars. Only sources with high SNR photometry are included. The fact that the CTTS, WTTS, and Herbig Ae/Be stellar populations appear to occupy different regions in Figure 1 enables us to pick out candidate PMS stars. The 2MASS database, with usually simultaneous measurements in all 3 bands, is particularly useful for a diagnostic of young stellar population based on colors, because a majority of PMS stars are variables.

Also shown in Fig. 1 is the locus for main sequence stars, for which the WTTS are seen to follow. The CTTS are found to lie approximately between the two parallel dotted lines, defined empirically by $(j_m - h_m) - 1.7(h_m - k_m) + 0.0976 = 0$ and $(j_m - h_m) - 1.7(h_m - k_m) + 0.450 = 0$, where j_m , h_m , and k_m are 2MASS magnitudes, and the slope is specified by the interstellar reddening law (Rieke & Lebofsky 1985). The dashed line in Fig. 1 represents the dereddened CTTS locus (Meyer et al. 1997), modified to the 2MASS photometry (Carpenter 2001), with $(j_m - h_m) - 0.493(h_m - k_m) - 0.439 = 0$. The dotted parallel lines separate CTTS from Herbig Ae/Be and from reddened main sequence stars. The fact that different kinds of PMS stars occupy separated regions in the $(J - H)$ versus $(H - K_S)$ color-color diagram enables us to identify candidate young stars in star-forming regions. We select 2MASS point sources with colors between the 2 parallel lines and above the dashed line as CTTS candidates. Inevitably our selection would miss some CTTS to the left of the parallel lines, where slightly reddened CTTS and reddened main sequence stars cannot be distinguished by their 2MASS colors. This poses no difficulty for our study because our goal is not to collect a complete PMS sample, but to use young stars as probes of the star formation history in the region. Data at longer wavelengths, e.g., at L band and beyond, would serve to better discriminate between moderately reddened CTTS and reddened main sequence stars (Lada et al. 2000).

To improve photometry accuracy and to remove extended sources from the 2MASS Point Source Catalog, we have set further criteria in selection of our CTTS candidates. These may be useful to other users of the 2MASS data, so we summarize them in Table 1. The Photometric quality flag (ph_qual = AAA) means $\text{SNR} \geq 10$, and with a corrected photometric

uncertainty less than 0.10857 mag, an indication of the best quality detection in terms of photometry and astrometry. The Blend flag (`bl_flg`) = 111 implies no source blending; the Contamination and Confusion flag (`cc_flg`) = 000 means the source is unaffected by known artifacts, or artifact is not detected in the band. Only sources without a neighboring star within 5'' (`prox` > 5.0'') are considered, so as to avoid possible photometric confusion. We select only sources which have optical counterparts (`a` ≠ 0) and identified CTTS candidates by the near-IR colors prescribed in the last paragraph.

Some slightly extended sources may be included in the 2MASS Point Source Catalog, notably nuclei of galaxies. In order to single out these non-stellar sources, additional criteria have been imposed. An extended source can be discriminated against a point source by the difference between its measured fluxes determined with a point-spread-function (PSF) fitting and with aperture photometry. Conceivably, an extended source measured by PSF photometry would lose some flux at the outer image halo. The 2MASS entries, `[j_hk_m]`, are default magnitudes mostly derived from PSF fitting, whereas the entries, `[j_hk_m_stdap]`, are standard aperture magnitudes derived from 4'' radius photometric aperture. Therefore the parameter $(j_m - j_m_stdap) + (h_m - h_m_stdap) + (k_m - k_m_stdap)$ should be close to 0 for point sources and significantly non-zero for extended objects. We set $(j_m - j_m_stdap) + (h_m - h_m_stdap) + (k_m - k_m_stdap) \leq 0.3$ as our selection criterion. Finally, we choose sources with SNR greater than 30 (`[j_hk]_snr` > 30) for high-quality photometry. These stringent criteria would bias against sources in crowded regions, but as shown below, prove to lead to a high success rate in selection of CTTS candidates.

In addition to 2MASS, we have made use of other survey data, such as the H α (Finkbeiner 2003; Gaustad et al. 2001), $E(B - V)$ reddening (Schlegel et al. 1998), and IRAS 100 μ m emission in the Orion star-forming region to trace, respectively, the distribution of ionization fronts, cloud extinction and IR radiation with respect to the spatial distribution of our sample of young stars.

2.2. SPECTROSCOPIC OBSERVATIONS

To justify the selection criteria outlined above, we have chosen 32 relatively bright CTTS candidates for spectroscopic observations to check their youth nature. Low-dispersion spectra, with dispersion of 200 Å/mm, 4.8 Å/pixel, were taken with the 2.16 m optical telescope of the Beijing Astronomical Observatory in 2003 January 22, 23, 30, and 31. An OMR (Optomechanics Research Inc.) spectrograph was used with a Tektronix 1024×1024 CCD detector covering 4000-9000 Å. The data were processed with standard NOAO/IRAF packages. After the bias and flat-fielding corrections, the IRAF package KPNOSLIT was

used to extract, and to calibrate the wavelength and flux of, each spectrum. Table 2 lists the results of our spectroscopic observations. The first column gives the sequence number. Columns 2–5 list the 2MASS identification and photometry. Columns 6–9 are, respectively, the spectral type, the associated star-forming region, forbidden line(s) in the spectrum if any, and other names for the source. We note that stars No. 3, 5, 6, 14, 15, 16, 20, 21, 22, and 24 in Table 2 show continuous or veiled spectra with [OI] and/or [SII] emission lines (Figure 3), characteristics of extreme T Tauri stars for which the forbidden lines originate from jets or winds seen commonly in Class I sources (Kenyon et al. 1998).

These 32 candidates, distributed between RA~5–6 h covering part of the Orion and part of the Monoceros star-forming regions, have been chosen somewhat randomly. Our spectroscopic observations show that 24 of the 32 candidates are found indeed to be pre-main sequence stars, with the other 4 as M-type stars and 4 as carbon stars. All 24 confirmed PMS stars are associated with star-forming regions, but otherwise the M stars and carbon stars are scattered around the region. This indicates that our criteria to select PMS stars from the 2MASS database are valid and very effective. If the same set of criteria are applied to sources seen against nearby molecular clouds — as is the case here in Orion and Monoceros bright-rimmed clouds — for which both background and foreground field star contamination is small, the success rate should be conceivably even higher.

Figure 4 shows the color-magnitude and color-color diagrams of the 24 spectroscopically confirmed CTTS in Table 2. Stars with and without forbidden lines are denoted with different symbols. In the color-magnitude diagram, the stellar absolute J magnitude, as the ordinate, is derived by adopting a distance of 450 pc to the Orion clouds and a distance of 830 pc to the Mon R2 and LDN 1652 star-forming regions (Maddalena et al. 1986). One sees that in either the color-magnitude diagram or the color-color diagram, the CTTS with forbidden lines are systematically further away from the zero-age main sequence (ZAMS), implying that the CTTS with forbidden lines are younger than those without.

This result, that younger CTTS are located to the upper-right corner in the near-infrared color-color diagram, is consistent with that obtained by Lada & Adams (1992). Class I sources, with very red colors, $(J - H) > 1.8$ mag, are located even more toward the upper-right corner in the diagram. In contrast, the WTTS are close to the main sequence locus, whereas the CTTS occupy a region between those of the Class I sources and the WTTS. This is understood as an evolutionary sequence; namely a young star evolves in such a color-color diagram from upper right to lower left, in a sequence from a Class I protostar, a CTTS with forbidden lines, a CTTS without forbidden, to a WTTS.

The spectroscopic observations demonstrate that our selection of PMS sample based on 2MASS colors is reliable, and that the color-magnitude diagram and color-color diagram

can be used, particularly for those CTTS too faint to obtain their spectra, to diagnose their evolutionary status. We are now ready to apply these tools to identify a sample of PMS stars in star-forming clouds, which in turn allows us to probe the star formation activity and history in the region.

3. EVIDENCE OF TRIGGERED STAR FORMATION

We present the analysis of the PMS population in relation with the bright-rimmed molecular clouds and massive stars to investigate how triggered star formation might have taken place. This paper concentrates on the Orion BRCs, IC 2118, LDN 1616, LDN 1634, and perhaps also Orion East, associated with the Trapezium, and B 30 and B 35 associated with the λ Orionis (Figure 2). The sample used in this study consists of (1) 33 CTTS candidates (including 2 confirmed CTTS in IC 2118 and 1 in LDN 1634, see Table 2) around the Trapezium, in the region $RA \sim 5^h$ to $5^h 30^m$, and $DEC \sim -2^\circ$ to -9° , and (2) 18 CTTS candidates around λ Orionis, in $RA \sim 5^h 25^m$ to $5^h 50^m$, and $DEC \sim +8^\circ$ to $+14^\circ$.

IC 2118, LDN 1616, and LDN 1634 are isolated molecular clouds to the west of the Orion A, as part of the Orion star-forming region. The 3 molecular clouds are all associated with strong IRAS $100 \mu m$ emission, and are apparently engraved by the UV radiation from the Trapezium, with the bright-rimmed boundaries, as outlined by $H\alpha$ filaments, presumably shaped by the I-fronts (Figure 5). We differentiate the CTTS physically close to the BRCs from those further away, as marked in Figure 5. The spectra of stars No. 14, 15 and 16, associated with IC 2118 and LDN 1634, all exhibit forbidden lines [S II] and/or [O I], suggestive of their youth. The spatial distribution of these CTTS likely traces a pre-existent molecular cloud complex for which IC 2118, LDN 1616, and LDN 1634 are merely survivors.

LDN 1621 and LDN 1622, also called Orion East (Herbig & Rao 1972), are at about the same distance as Orion B (Maddalena et al. 1986). Interaction between the Orion East clouds and the I-front can be seen in Figure 6.

B 30 and B 35 are associated with S 264, an extended H II region excited by the O8 III star λ Orionis and surrounded by, but slightly off centered of, a ring molecular cloud (Lang et al. 2000). Duerr et al. (1982) have surveyed about 100 square degrees around λ Orionis, and found 83 $H\alpha$ emission-line stars, mostly distributed along a bar-like structure extending on either side from λ Orionis to B 30 and to B 35. These authors suggest that the $H\alpha$ stars provide a fossil record of a pre-existent giant molecular cloud complex. Dolan & Mathieu (2002) have identified PMS stars in the region around λ Orionis by statistical removal of field stars in the optical color-magnitude diagram. The seeming lack of the youngest (1-2

Myr) PMS stars inside the molecular ring, despite the apparent abundance of such stars in B 30 and B 35, leads Dolan & Mathieu (2002) to postulate a possible supernova explosion near λ Orionis that terminated recent star formation in the vicinity. The CTTS candidates we have identified spread along the bar-like structure, but clearly within the central cavity previously thought to be free of ongoing star-forming activities. Prominent $H\alpha$ and IRAS 100 μm emission are seen in both B 30 and B 35 on the sides facing λ Orionis (Figure 7), signifying the interaction between λ Orionis and these two BRCs.

3.1. COMPARISON WITH THEORY

The radiation-driven implosion (RDI) model, based on the “rocket effect”, proposed by Oort & Spitzer (1955) and further developed by Bertoldi (1989) and by Bertoldi & McKee (1990), links BRCs to PMS stars. The UV photons from massive stars ionize the outer layers of a nearby cloud, which expand to the surrounding medium with an I-front speed $\sim 10 \text{ km s}^{-1}$. The expanding I-front plows the cloud material which, when exceeding the local critical mass, collapses to form new stars. There are two phases, namely collapsing and cometary phases, for the formation and evolution of a cometary globule (Lefloch & Lazareff 1994, 1995; Lefloch et al. 1997). In the initial collapsing phase, the UV photons ionize the surface layers of a cloud, causing the cloud to elongate in the direction of the high-mass stars. This phase lasts some 10^5 yr . Subsequently, the cloud would remain in a quasi-stationary state, with small-scale condensations close to critical equilibria. If the I-front out-pressures the molecular cloud, the density increases to beyond the critical value and the collapse of the condensations leads to star formation, leaving behind a chain of PMS stars reminiscent of the original, elongated cloud. On the other hand, if the I-front does not out-pressure the molecular gas, the I-front stalls and there should be no star forming. This cometary phase may last a few million to a few 10^7 years . Eventually the entire cometary globule would be evaporated by the UV photons.

According to the RDI model, the surface of a BRC facing the massive stars is compressed by the I-fronts. De Vries et al. (2002) observed B 35 and LDN 1634 in HCO^+ and other molecular line transitions to trace the swept-up gas ridge and overly dense regions. They find that the surfaces of B 35 and LDN 1634 facing the massive stars are indeed being compressed, as the RDI model predicts.

Ogura & Sugitani (1998) listed several dozens of bright-rimmed clouds, cometary globules and reflection clouds in the Orion OB1. They propose these present an evolutionary sequence and collectively call them “remnant molecular clouds”. We find that not all remnant molecular clouds are associated with CTTS. Instead, only those BRCs associated with

prominent $H\alpha$ and IRAS 100 μm emission, e.g., IC 2188, LDN 1616, and LDN 1634, have ongoing star formation (Figure 8), consistent with the RDI model. The $H\alpha$ filaments and the 100 μm emission trace, respectively, the I-fronts and dense regions in a molecular cloud. Obviously in IC 2188, LDN 1616, and LDN 1634, the I-front has out-pressured the molecular clouds and thus triggered star formation. The two BRCs B 30 and B 35 in the vicinity of λ Orionis are additional two such examples of triggered star formation. Remnant clouds without star formation are simply the outcome of I-fronts with insufficient pressure.

The RDI model predicts the cloud to collapse perpendicular to the direction of the ionizing massive stars. This has been observed in LDN 1616 and IC 2118 by Yonekura et al. (1999), for which the ^{12}CO , ^{13}CO , and C^{18}O emission contours show elongation roughly toward the Trapezium.

3.2. SEQUENTIAL STAR FORMATION

Triggered star formation is a sequential process. Massive stars form first, and their I-fronts expand to and compress nearby molecular clouds, prompting the next-generation stars to form. The process may continue until the cloud is consumed and no more star-forming material is available. As time passes, the PMS stars would line up between the massive stars and the molecular cloud, along which the stars farther away from the massive stars, and thus closer to the molecular cloud, should be progressively younger. The youngest stellar objects, namely protostars (Class 0 and Class I objects, Lada 1987), would still be embedded within the cloud.

Our data indicate a systematic brightness difference among revealed CTTS, in the sense that brighter CTTS are more distant from λ Orionis (cf. Fig. 7). We consider this as the consequence of triggered star formation. Initially, the B 30 and B 35 clouds might have been extended toward λ Orionis, perhaps with a bar-like structure (Duerr et al. 1982). The I-front from λ Orionis propagates and rams through the clouds, leaving behind newborn stars. Figure 10 plots the color-magnitude diagram in the λ Orionis region. Indeed the CTTS closer to B 30 and B 35 are progressively younger, and away from zero-age main sequence (Siess et al. 2000). The brightest CTTS, close to B 30 and B 35, may be among the youngest which have just revealed themselves on the birthline and begun their descent down the Hayashi tracks. The same phenomenon, namely the CTTS closer to the BRCs are perceptibly younger, is seen in LDN 1616, LDN 1634, and IC 2118 (Fig. 9). The star formation sequence is similar, except here with the Trapezium as the triggering source.

Figure 10 also shows the color-color diagram of the λ Orionis region, in which the CTTS

physically closer to BRCs are located to the upper-right corner. The extinction values in these BRCs, derived from Schlegel et al. (1998), are in general too low to affect the apparent colors significantly. This implies these CTTS are intrinsically young. In LDN 1616, LDN 1634, and IC 2118, we also find similar results as in the λ Orionis region (cf. Fig. 9).

Some very young objects are known to exist in these regions, for example with Class 0 sources in B 30 (RNO 43MM, Zinnecker et al. 1992) and in LDN 1616 (L 1616 MMS1A, Stanke et al. 2002), and with Class I sources in B 35 and in LDN 1634 (De Vries et al. 2002). Each of them is indeed embedded in, and close to the apex of, the associated cloud, as expected in the RDI model. We are apparently witnessing an ongoing star formation sequence, with coexistence of CTTS, younger PMS associated with BRCs, to the youngest protostars embedded within the clouds.

3.3. RELEVANT TIMESCALES

In the triggered star-formation scenario, the ages of the concurrent OB stars must be longer than the ages of the second-generation stars plus the I-front traveling time. The stars $^1\theta$ Ori A, B, C, and D, with spectral types B0.5V, B3V, O6:, and B0.5V, respectively (Levato & Abt 1976), are the most massive members in the Trapezium and the main sources to create the I-fronts. The star $^1\theta$ Ori C may be somewhat peculiar in its evolutionary status (Walborn & Panek 1984), so we adopt the age of $^1\theta$ Ori A and D, both of spectral type B0.5V with a lifetime of 6×10^6 yr (Schaerer & de Koter 1997) to represent the ages of the OB stars.

Assuming IC 2118, LDN 1616, and the Trapezium are at the same distance from us, IC 2118 and LDN 1616 are thus separated from the Trapezium by about 55 pc. With an I-front speed, i.e., the sound speed in an HII region, ~ 10 km s $^{-1}$, it takes some 5.5×10^6 yr for the I-front to traverse. The lifetimes of CTTS range from a few 10^5 to a few 10^6 yr. The CTTS associated with the BRCs are younger than those outside the clouds (§3.2), but even for the oldest CTTS in the region, the combined timescale 6×10^6 yr is consistent with the age of the Trapezium.

Likewise, the set of timescales can be estimated for the λ Orionis system, which consists of an O star and an HII region surrounded by an unusual molecular cloud ring. The radius of the molecular cloud ring is approximately 2.6 deg, or about 20 pc at 450 pc distance, so it would take about 2 Myr for the I-front, originated from λ Ori, to travel through the HII region. The age of λ Orionis, an O8III star with a luminosity of 340,000 L_{\odot} and an effective temperature of 34,700 K (Schmidt-Kaler 1982) can be inferred from evolutionary

tracks (Schaerer & de Koter 1997) to be about 3×10^6 yr. Here again, the age of the triggerer λ Orionis (3×10^6 yr) is consistently longer than the expanding timescale of I-front (2×10^6 yr) plus the age of the CTTS.

3.4. SPATIAL DISTRIBUTION OF CLASSICAL T TAURI STARS

The spatial distribution of CTTS provides telltale clues to the star formation history in a molecular cloud. According to the RDI model, small-scale condensations compressed by the I-fronts would reach critical equilibria first at the surface layers of BRCs, where the CTTS should be found. If CTTS exist far ahead of the I-front and are still embedded in the molecular cloud, the star formation must have proceeded in a spontaneous manner, i.e. the embedded CTTS were formed at the same time with their massive counterparts. On the other hand, if CTTS are only seen near the surfaces of — and none embedded inside — the BRCs, triggered star formation is clearly evinced. In B 30, B 35, IC 2118, LDN 1616, LDN 1634 and Orion East, CTTS are seen only between the massive stars and BRCs, and on the compressed (i.e., dense) sides of BRCs (see Figure 5, 6, and 7). No CTTS are found further down the compressed regions into the molecular clouds.

To investigate if the BRCs are indeed void of embedded PMS stars, we have computed the probability of our failure to detect them, if they actually existed, because of excessive dust extinction in the clouds. Table 3 contains the extinction of IC 2118, LDN 1616, LDN 1634, B 30, and B 35. Column 1 lists the 5 BRCs. Columns 2 to 4 are the $E(B - V)$, A_V , and A_J in each cloud. The values of $E(B - V)$ are derived from Schlegel et al. (1998), and $A_V/E_{B-V}=3.1$ and $A_J = 0.282A_V$ (Cox 1999) are used to obtain A_V and A_J . If there were CTTS embedded in a particular cloud, we would like to estimate how many of them would have hidden from our detection. We created the $E(B - V)$ map (Schlegel et al. 1998) for each cloud, and assumed the same J band luminosities for the embedded CTTS as those for the visible CTTS outside the cloud. We performed Monte Carlo computation to distribute randomly the hypothetical CTTS stars on the $E(B - V)$ map to check their detectability, given the 2MASS detection limit of $J = 15.0$ (SNR=30) based on selection criteria discussed in § 2. The probability of non-detection of embedded CTTS in each cloud is given as Column 5. As can be seen, the probability of CTTS that would have escaped our detection is universally very low, < 0.06 , implying that the extinction in these clouds is too low to make any embedded PMS stars invisible. In other words, if there were any embedded sources, we would have detected them. We conclude therefore that the CTTS near the surfaces of the BRCs are not part of a young stellar population originally embedded in the molecular clouds and later revealed by UV photons from massive stars. They are

relics of triggered star formation.

Most PMS stars are associated with molecular clouds, but some are distinctly away from any clouds. These isolated PMS stars, with their juvenility, could not have traversed from the birthplace to their current positions. They are revealed as a consequence of surplus star-forming material being stripped off by radiation and winds from nearby massive stars, leaving behind PMS stars away from molecular clouds.

3.5. HIGH STAR FORMATION EFFICIENCY

Massive stars play a dual role in star formation. The I-front compression may induce birth of stars which otherwise could not have formed. Alternatively molecular clouds may become highly disturbed, hence dispersed, making subsequent star formation impossible. Even if triggered star formation is initiated, the working is confined to the outer layers of a cloud. It is therefore expected that star formation may be efficient in localized, compressed regions, but perhaps not so in the entire cloud. The star formation efficiency (SFE) in a BRC can be estimated by the ratio of stellar mass to the total mass of stars plus cloud. De Vries et al. (2002) observed the compressed regions of B 35 and LDN 1634 in the HCO^+ molecular line and determined the total compressed mass of molecular clouds to be $27 M_\odot$ for B 35 and $28 M_\odot$ for LDN 1634, respectively. We have identified 3 CTTS in each of B 35 and LDN 1634, so assuming $0.5\text{--}1 M_\odot$ for a typical CTTS, the SFEs of the compressed material in B 35 and in LDN 1634 are about 5–10%, higher than that of a few percent ($< 3\%$) in other nearby star-forming regions (White et al. 1995).

4. CONCLUSIONS

We have developed an empirical set of criteria to select candidate classical T Tauri stars on the basis of the infrared colors in the 2MASS Point Source Catalog. Among the 32 candidates we have obtained the spectra, 24 are found to be bona fide PMS objects, 4 are M-type stars and the rest 4 are carbon stars, which shows the effectiveness of our selection method. The young stellar population provides a tool to trace ongoing star formation activities. We find supportive evidence of triggered star formation in the following bright-rimmed clouds, B 35, B 30, IC 2118, LDN 1616, LDN 1634, and Orion East.

1. Our data supports the radiation-driven implosion model that links the formation of BRCs and of stars. The ionization fronts from OB stars compress a nearby cloud, and if the density of the compressed gas exceeds a certain critical value, new stars would be

formed. Not all BRCs are associated with CTTS. Only BRCs associated with strong IRAS 100 μm emission (tracer of high density) and $\text{H}\alpha$ emission (tracer of ionization front) show signs of ongoing star formation.

2. We find that CTTS closer to BRCs are progressively younger, a configuration consistent with the sequential process of triggered star formation. The brightest CTTS, spatially closest to BRCs, are the young stellar objects which just reveal themselves on the birthline and begin to descend down the Hayashi tracks.
3. The ages of the concurrent OB stars are comparable or older than the ages of the next-generation stars plus the I-front traveling times. These timescales are consistent with the causality, or sequential, nature of the star formation process.
4. CTTS are found only in between the OB stars and the molecular clouds with which the ionization fronts interact. There are no CTTS ahead of the ionization fronts into the clouds. The lack of embedded CTTS cannot be due to detection sensitivity because the extinction of these BRCs is generally low.
5. Current star formation in the BRCs takes place in the compressed outer layers of the molecular clouds. The relatively enhanced star formation efficiency suggests a triggering—as opposed to a spontaneous—star formation process.

This research makes use of data products from the Two-Micron All-Sky Survey, which is a joint project of the University of Massachusetts and the Infrared Processing and Analysis Center/California Institute of Technology, funded by the National Aeronautics and Space Administration and the National Science Foundation. We also use the Southern H-Alpha Sky Survey Atlas (SHASSA), supported by the National Science Foundation. We are grateful to the anonymous referee for helpful suggestions that improve the quality of his paper. We also thank the staff at the Beijing Astronomical Observatory for their assistance during our observing runs. Hsu-Tai Lee wants to thank Paul Ho for valuable discussions. We acknowledge the financial support of the grants NSC92-2112-M-008-047 of the National Science Council, and 92-N-FA01-1-4-5 of the Ministry of Education of Taiwan.

REFERENCES

- Carpenter, J. M. 2001, *AJ*, 121, 2851
- Bertoldi, F. 1989, *ApJ*, 346, 735
- Bertoldi, F. & McKee, C. F. 1990, *ApJ*, 354, 529
- Cox, A. N. 1999, *Allens Astrophysical Quantities*
- De Vries, C. H., Narayanan, G., & Snell, R. L. 2002, *ApJ*, 577, 798
- Dolan, C. J., & Mathieu, R. D. 2002, *AJ*, 123, 387
- Duerr, R., Imhoff, C. L., & Lada, C. J. 1982, *ApJ*, 261, 135
- Elmegreen, B. G. 1998, *ASP Conf. Ser.* 148: *Origins*, 150
- Feigelson, E. D., & Montmerle, T. 1999, *ARA&A*, 37, 363
- Finkbeiner, D. P. 2003, *ApJS*, 146, 407
- Gaustad, J. E., McCullough, P. R., Rosing, W., & Van Buren, D. 2001, *PASP*, 113, 1326
- Herbig, G. H. & Bell, K. R. 1988, *Lick Observatory Bulletin*, Santa Cruz: Lick Observatory, c1988,
- Herbig, G. H. & Kameswara Rao, N. 1972, *ApJ*, 174, 401
- Karr, J. L., & Martin, P. G. 2003, *ApJ*, 595, 900
- Kenyon, S. J., Brown, D. I., Tout, C. A., & Berlind, P. 1998, *AJ*, 115, 2491
- Lada, C. J., Muench, A. A., Haisch, K. E., Lada, E. A., Alves, J. F., Tollestrup, E. V., & Willner, S. P. 2000, *AJ*, 120, 3162
- Lada, C. J. 1987, *IAU Symp.* 115: *Star Forming Regions*, 115, 1
- Lada, C. J., & Adams, F. C. 1992, *ApJ*, 393, 278
- Lang, W. J., Mashedier, M. R. W., Dame, T. M., & Thaddeus, P. 2000, *A&A*, 357, 1001
- Lefloch, B. & Lazareff, B. 1994, *A&A*, 289, 559
- Lefloch, B. & Lazareff, B. 1995, *A&A*, 301, 522
- Lefloch, B., Lazareff, B., & Castets, A. 1997, *A&A*, 324, 249

- Levato, H. & Abt, H. A. 1976, PASP, 88, 712
- Maddalena, R. J., Moscovitz, J., Thaddeus, P., & Morris, M. 1986, ApJ, 303, 375
- Meyer, M. R., Calvet, N., & Hillenbrand, L. A. 1997, AJ, 114, 288
- Oort, J. H. & Spitzer, L. J. 1955, ApJ, 121, 6
- Ogura, K. & Sugitani, K. 1998, PASA, 15, 91
- Rieke, G. H. & Lebofsky, M. J. 1985, ApJ, 288, 618
- Schaerer, D. & de Koter, A. 1997, A&A, 322, 598
- Schlegel, D. J., Finkbeiner, D. P., & Davis, M. 1998, ApJ, 500, 525
- Schmidt-Kaler, T. 1982, Landölt-Bornstein Numerical Data and Functional Relationships in Science and Technology
- Siess, L., Dufour, E., & Forestini, M. 2000, A&A, 358, 593
- Stanke, T., Smith, M. D., Gredel, R., & Szokoly, G. 2002, A&A, 393, 251
- Sugitani, K., Fukui, Y., & Ogura, K. 1991, ApJS, 77, 59
- Sugitani, K., & Ogura, K. 1994, ApJS, 92, 163
- Thé, P. S., de Winter, D. & Pérez, M. R. 1994 A&AS, 104, 315
- Walborn, N. R. & Panek, R. J. 1984, ApJ, 286, 718
- White, G. J., Casali, M. M., & Eiroa, C. 1995, A&A, 298, 594
- Wichmann, R. et al. 1996, A&A, 312, 439
- Yonekura, Y., Hayakawa, T., Mizuno, N., Mine, Y., Mizuno, A., Ogawa, H., & Fukui, Y. 1999, PASJ, 51, 837
- Zinnecker, H., Bastien, P., Arcoragi, J., & Yorke, H. W. 1992, A&A, 265, 726

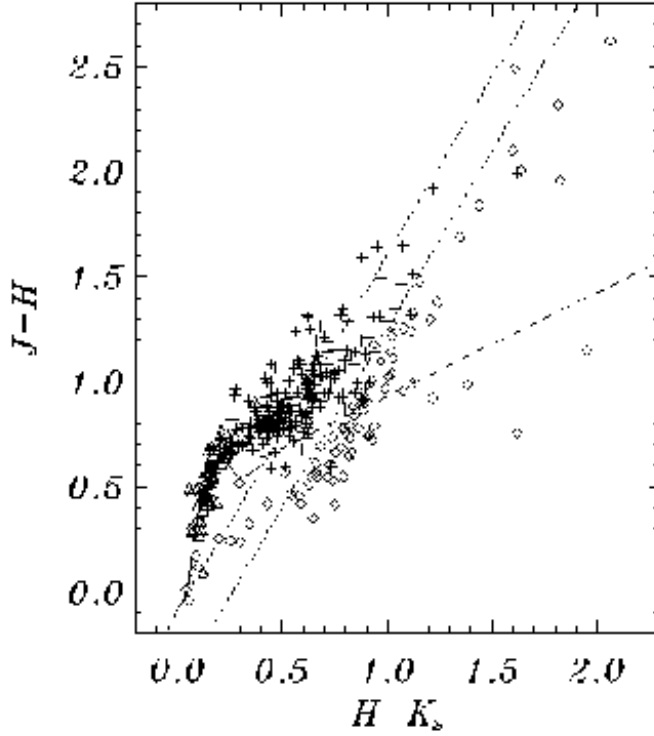


Fig. 1.— The 2MASS JHK color-color diagram for known WTTS ((Wichmann et al. 1996), triangles), CTTS ((Herbig & Bell 1988), pluses) and Herbig Ae/Be stars ((Thé et al. 1994), diamonds). The solid line is the main sequence locus. The two dotted parallel lines, with the slope derived from interstellar reddening law (Rieke & Lebofsky 1985), separate CTTS from Herbig Ae/Be and from reddened main sequence stars. The dashed line is the dereddened CTTS locus (Meyer et al. 1997).

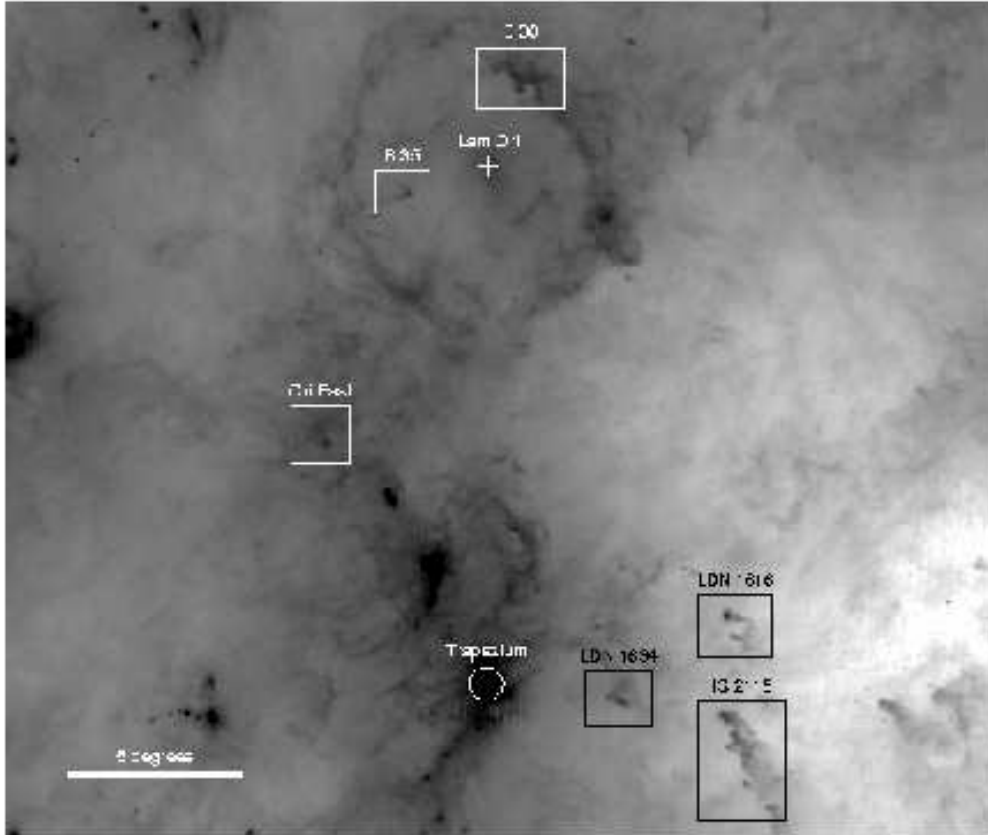


Fig. 2.— IRAS 100 μm image of the Orion region with the 6 bright-rimmed clouds studied in this work, B 30, B 35, Orion East, LDN 1616, LDN 1634, and IC 2118.

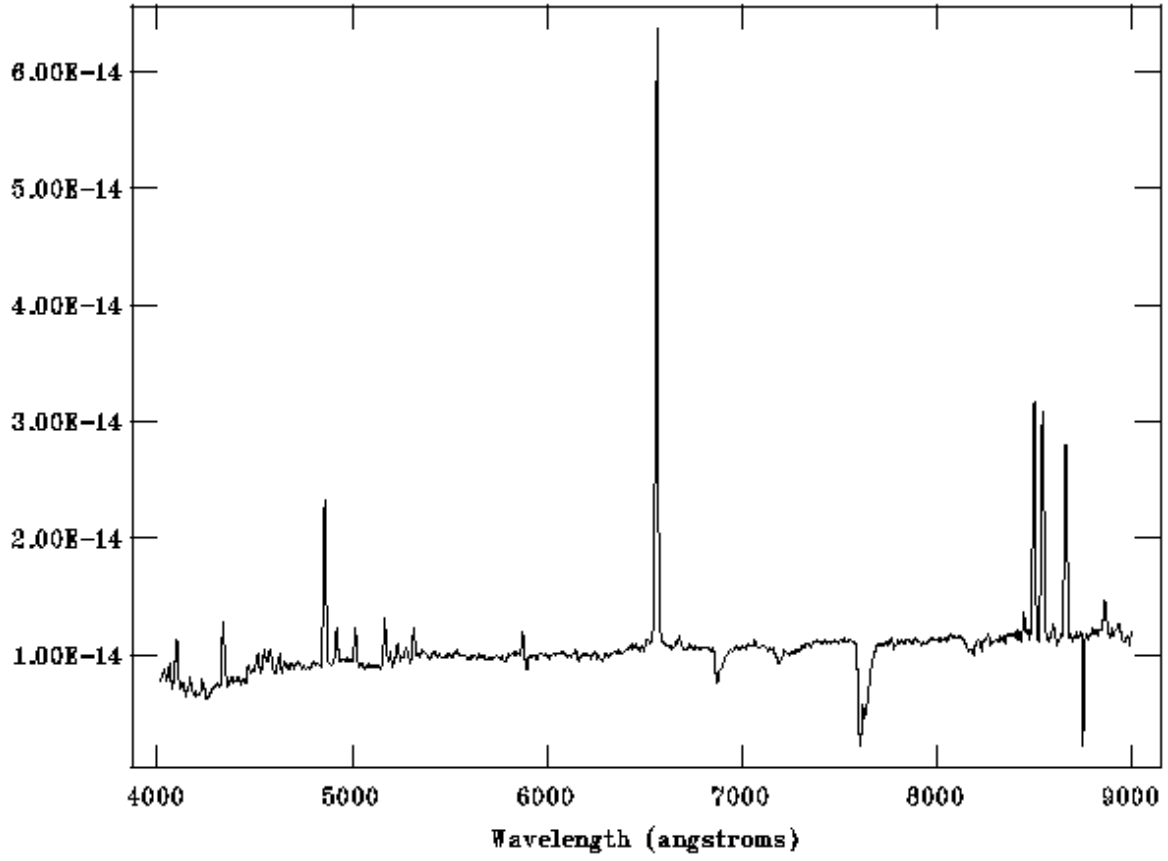


Fig. 3.— Example CTTS spectrum for star No.16 showing extreme CTTS characteristics of a veiled continuum with strong $H\alpha$, CaII triplets and forbidden [O I] and [S II] lines.

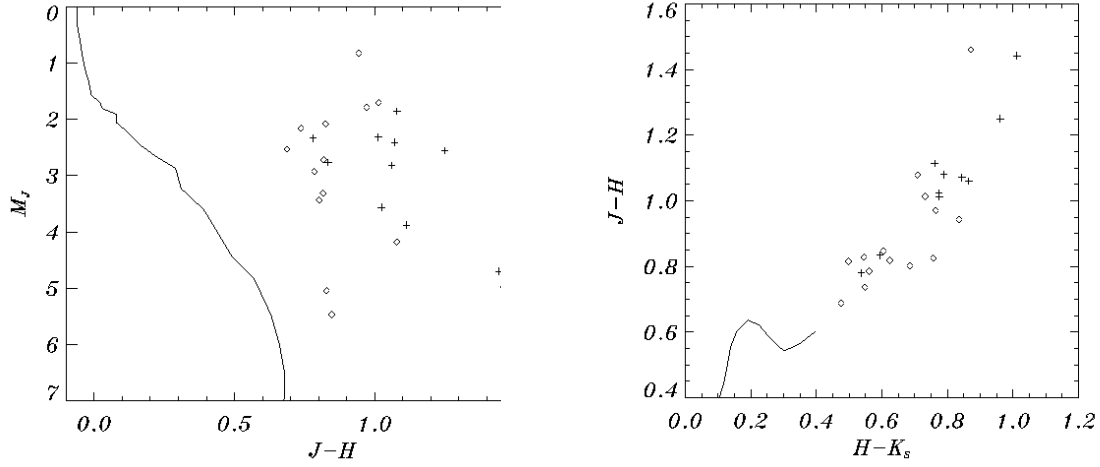


Fig. 4.— Color-magnitude diagram and color-color diagram for the 24 verified CTTS in Table 2 with (pluses) and without (diamonds) optical forbidden lines. In the color-magnitude diagram the solid line represents the ZAMS. In the color-color diagram the solid line is the main sequence locus. In either case, the CTTS with forbidden lines are further way from the main sequence, suggestive of their redder colors and younger ages than those without forbidden lines.

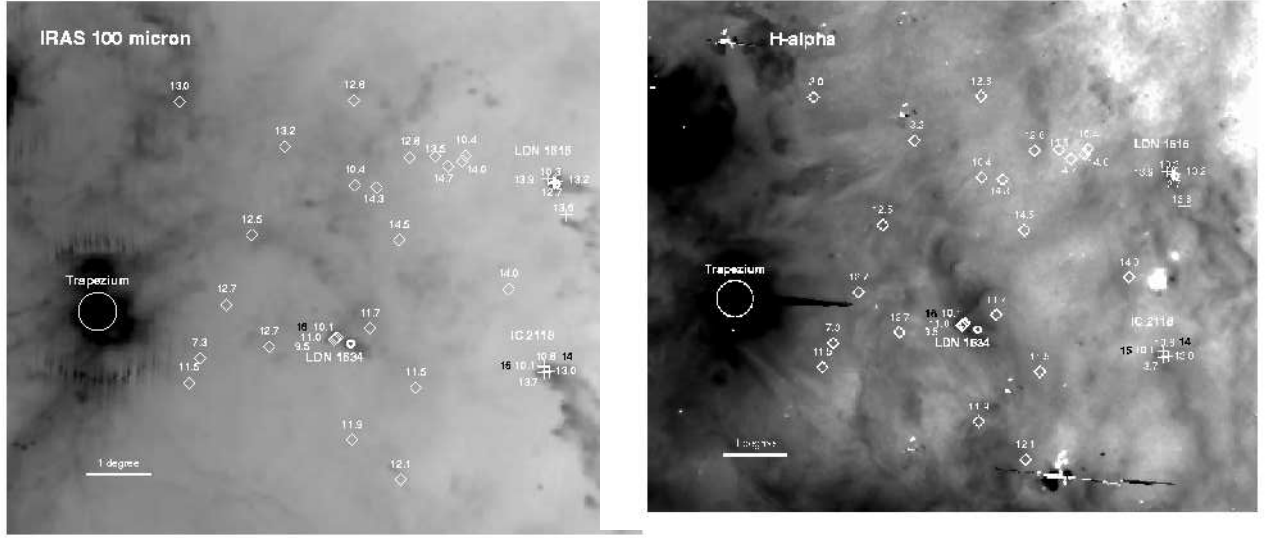


Fig. 5.— IRAS 100 μm and $\text{H}\alpha$ images in IC 2118, LDN 1616, and LDN 1634. There are a total of 33 CTTS candidates in the region. The pluses denote those CTTS physically closer to the BRCs, and the diamonds are those further away, with the J-band magnitude labeled for each star. Stars No. 14, 15 and 16 in Table 2 are labeled in black. The circles mark the positions of known protostars in the clouds (see §3.2).

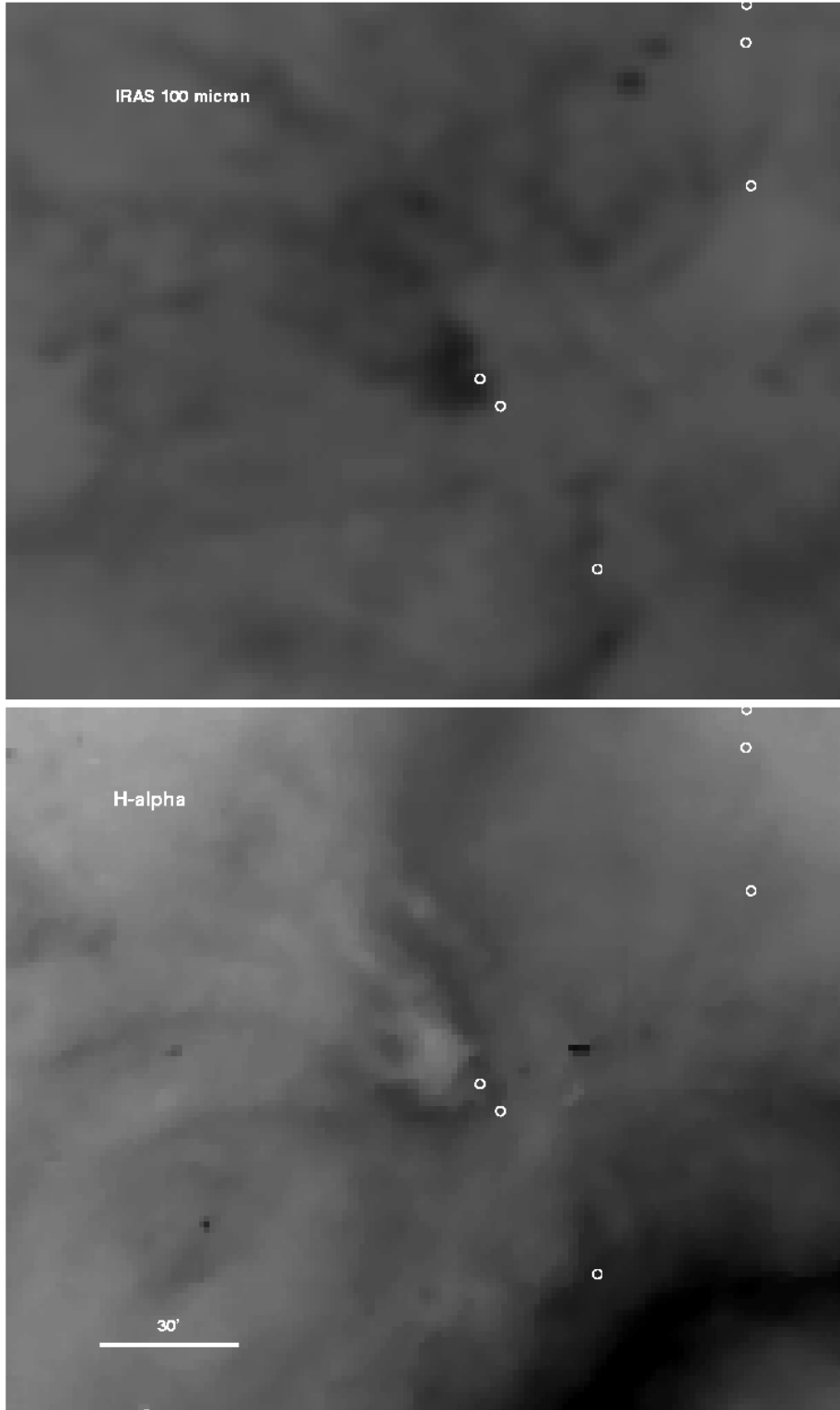


Fig. 6.— IRAS 100 μm and $\text{H}\alpha$ images of Orion East, with candidate CTTS marked.

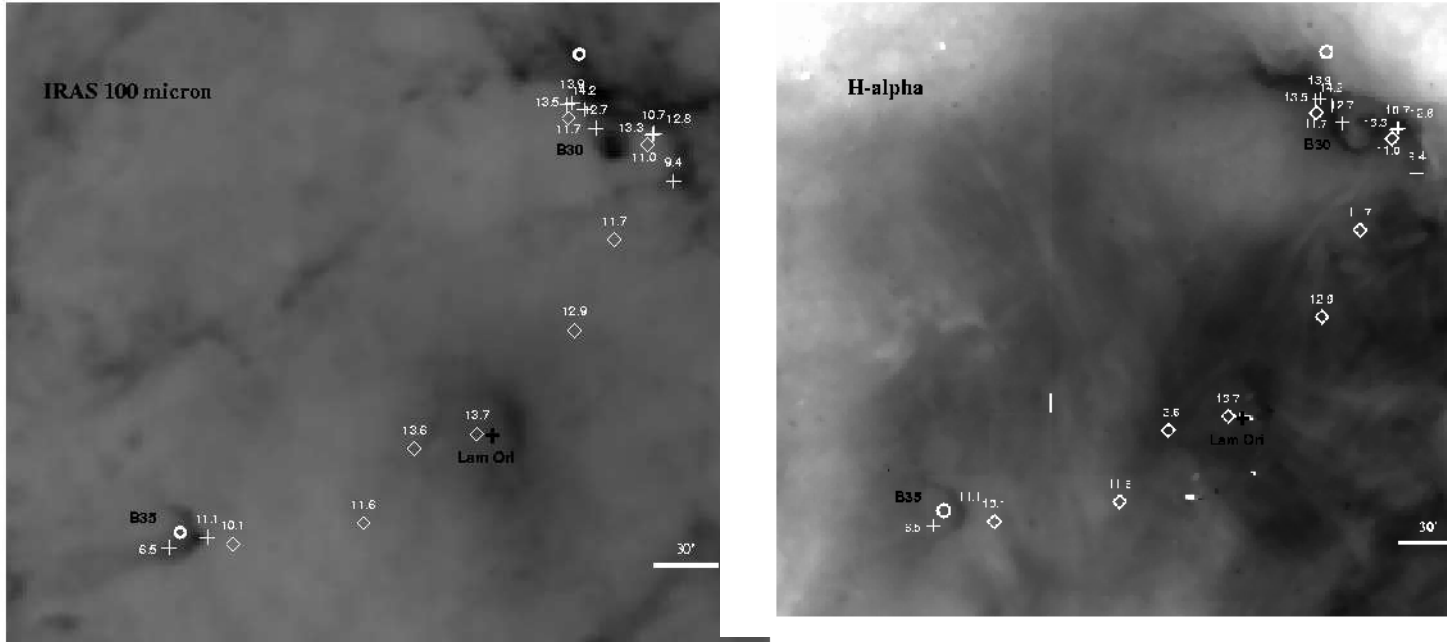


Fig. 7.— Same as Fig. 5 but for B 30 and B 35. There are a total of 18 CTTS candidates in the region.

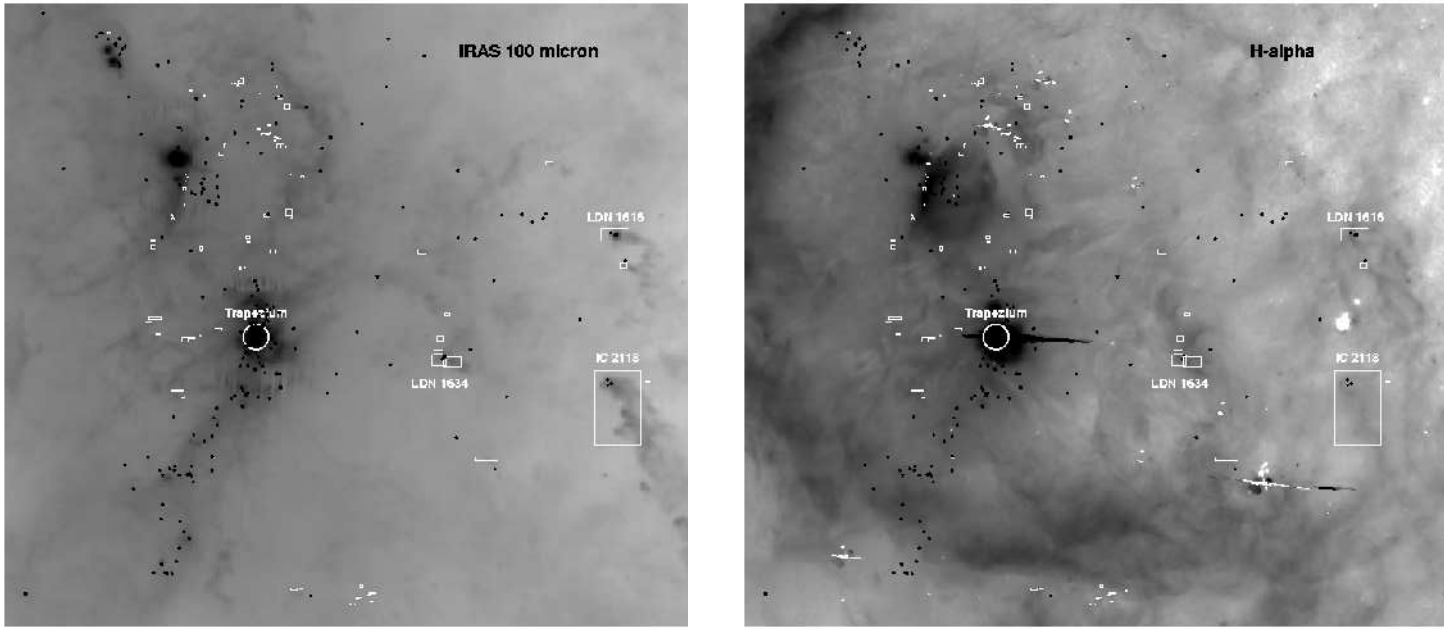


Fig. 8.— IRAS 100 μm and $\text{H}\alpha$ images of remnant molecular clouds. The white boxes are the remnant molecular clouds (Ogura & Sugitani 1998), and the black dots symbolize the candidate CTTS. Only clouds associated with strong IR and $\text{H}\alpha$ emission are found to harbor CTTS.

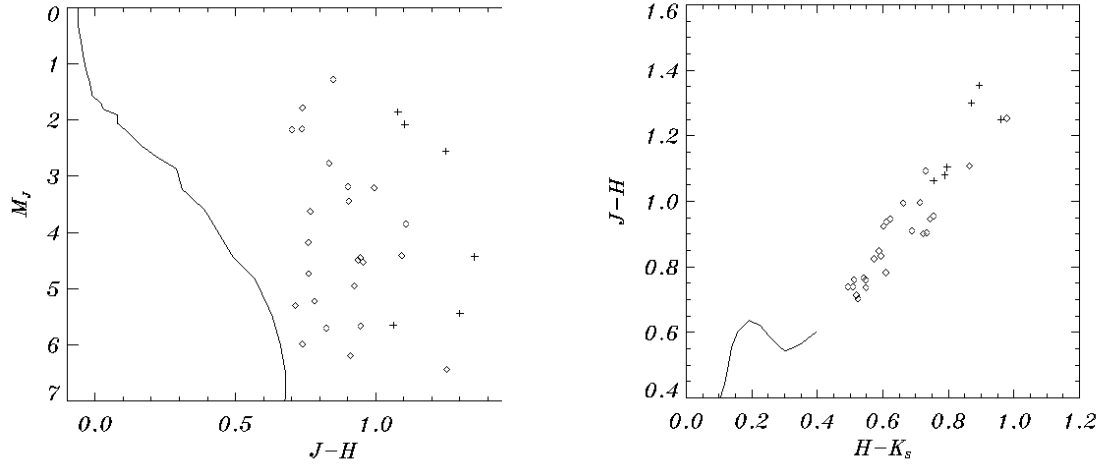


Fig. 9.— Color-magnitude and color-color diagrams of IC 2118, LDN 1616, and LDN 1634. In the color-magnitude diagram the solid line represents the ZAMS. In the color-color diagram the solid line is the main sequence locus. The CTTS physically closer to BRCs are marked with pluses, and those further away are marked with diamonds (cf. Fig. 5).

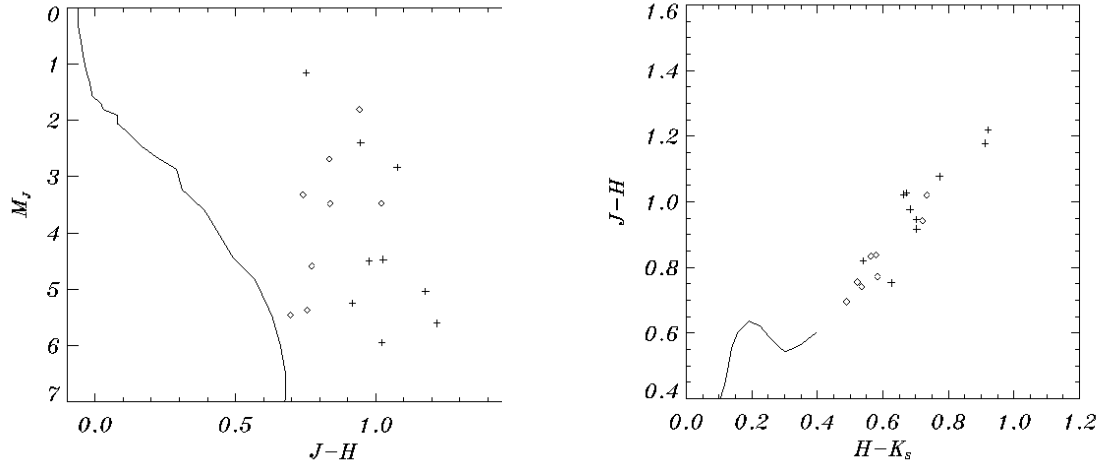


Fig. 10.— Same as Fig. 9 but for the B30 and B35 region (cf. Fig. 7.)

Table 1. Selection Criteria of CTTS from 2MASS Point Source Catalog

Criterion	Description
Photometric quality flag (ph_qual) = AAA	$SNR \geq 10$ and $[jhk]_{cmsig} < 0.10857$ for best-quality detections in photometry and astrometry
Blend flag (bl_flg) = 111	No source blending
Contamination and confusion flag (cc_flg) = 000	Source unaffected by known artifacts
Proximity (prox) $> 5.0''$	Photometry not confused by nearby objects
Minor Planet Flag (mp_flg) = 0	Not a minor planet
$(j_m - j_m_stdap) + (h_m - h_m_stdap) + (k_m - k_m_stdap) \leq 0.3mag$	To distinguish an extended source from a point source
$(j_m - h_m) - 1.7(h_m - k_m) + 0.0976 \leq 0$	2MASS colors of CTTS
$(j_m - h_m) - 1.7(h_m - k_m) + 0.4500 \geq 0$	
$(j_m - h_m) - 0.493(h_m - k_m) - 0.439 \geq 0$	
Optical counterpart (a) $\neq 0$	With an optical counterpart
signal-to-noise ratio ($[jhk]_{snr}$) > 30	$SNR > 30$

Table 2. Spectroscopic Observations of Young Star Candidates

Star	2MASS	J (mag)	H (mag)	K_S (mag)	Sp. Type ^a	Region Region	Forbidden Lines Line ^b	Other Name
1	J05350900-0427510	10.797	10.109	9.634	K0	Orion A	-	[R2001] 1754
2	J05353672-0510004	13.309	12.481	11.936	M3	Orion A	-	[AD95] 1868
3	J05385149-0801275	12.967	11.525	10.513	M5	Orion A	O, S	
4	J05402496-0755353	12.446	11.367	10.658	M4	Orion A	-	
5	J05412534-0805547	10.604	9.824	9.287	Cont.	Orion A	O	HBC 181
6	J05412771-0931414	12.147	11.033	10.272	Cont.	Orion A	O	Kiso A-1048 45
7	J05423584-0958552	9.973	8.959	8.227	Cont.	Orion A	-	
8	J05432701-0959375	10.984	10.166	9.542	K5	Orion A	-	
9	J05342764-0457051	13.737	12.890	12.286	M2	Orion A	-	[CHS2001] 3990
10	J05342978-0451477	13.241	11.781	10.910	K7	Orion A	-	[CHS2001] 4167
11	J05122053-0255523	10.425	9.688	9.140	K3	-	-	V531 Ori
12	J05371885-0020416	11.577	10.761	10.263	K5	-	-	Kiso A-0904 58
13	J06014515-1413337	11.698	10.896	10.211	K5	-	-	IRAS 05594-1413
14	J05073016-0610158	10.822	9.572	8.611	M0	IC 2118	O, S	
15	J05073060-0610597	10.120	9.040	8.251	M2	IC 2118	O	
16	J05202573-0547063	11.036	10.202	9.608	Cont.	LDN 1634	O, S	V534 Ori
17	J06075243-0516036	10.417	9.474	8.639	K0	Mon R2		HBC 518
18	J06075463-0614342	11.676	10.851	10.094	K0	Mon R2	-	
19	J06080003-0519022	11.384	10.413	9.649	K0	Mon R2	-	
20	J06261259-1028346	12.412	11.352	10.487	Cont.	LDN 1652	O, S	
21	J06265529-0958014	11.914	10.901	10.126	Cont.	LDN 1652	O	
22	J06265731-0959395	13.161	12.137	11.363	Cont.	LDN 1652	O	
23	J06273428-1002397	12.522	11.737	11.176	K7	LDN 1652	-	
24	J06280028-1003420	12.006	10.935	10.091	Cont.	LDN 1652	O	
25	J05375005-1548114	6.573	5.571	4.912	M9	-	-	IRAS 05355-1549
26	J06222376-0255509	10.410	8.734	7.559	C	-	-	IRAS 06198-0254

Table 2—Continued

Star	2MASS	<i>J</i>	<i>H</i>	<i>K_S</i>	Sp. Type ^a	Region Region	Forbidden Lines Line ^b	Other Name
		(mag)	(mag)	(mag)				
27	J06380179-0557170	8.000	6.711	5.841	C	-	-	
28	J06270654-0540512	8.082	6.751	5.882	C	-	-	
29	J06160006-1727270	10.213	8.978	8.040	C	-	-	
30	J06265037-0738456	9.830	8.845	8.543	M2	-	-	
31	J05345877-0928274	7.700	6.818	6.295	M9	-	-	V653 Ori
32	J05413322-0755022	12.209	11.174	10.526	M2	-	-	Haro 4-488

^aCont.–continuum spectra; C–carbon star

^bO–[O I] ;S–[S II]

Table 3. EXTINCTION OF BRIGHT-RIMMED CLOUDS

BRC	$E(B - V)^a$ (mag)	$A_V(R = 3.1)$ (mag)	A_J (mag)	Nondetection Prob.
IC 2118	1.1–0.2	3.4–0.6	0.96–0.17	0.021
LDN 1616	2.3–0.2	7.1–0.6	2.01–0.17	0.051
LDN 1634	1.1–0.3	3.1–0.9	0.87–0.25	0.013
B 30	2.6–1.5	8.1–4.7	2.28–1.31	0.058
B 35	1.3–0.5	4.0–1.6	1.14–0.44	0.001

^aSchlegel et al. (1998)